JOURNAL OF CATALYSIS 85, 437–456 (1984)

Decomposition of Methanol, Formaldehyde, and Formic Acid on Nonpolar ($10\bar{1}0$), Stepped ($50\bar{5}1$), and (0001) Surfaces of ZnO by Temperature-Programmed Decomposition

S. AKHTER, W. H. CHENG, K. LUI, AND H. H. KUNG[1]

Chemical Engineering Department and the Ipatieff Laboratory, Northwestern University, Evanston, Illinois 60201

Received March 18, 1983; revised August 25, 1983

The decompositions of methanol, formaldehyde, and formic acid were studied on a nonpolar ($10\bar{1}0$), a stepped ($50\bar{5}1$), and a Zn polar (0001) surface by temperature-programmed decomposition. The decomposition products on the ($10\bar{1}0$) and the ($50\bar{5}1$) surfaces were similar, but the coverage and the amount of products were consistently higher on the ($50\bar{5}1$) surface. On these two surfaces, methanol decomposed in two pathways. In one pathway, dissociatively adsorbed methanol decomposed into methane and adsorbed oxygen at 150°C. In the other pathway, the methoxide was oxidized to a surface formate-like species which decomposed at 380°C into CO, CO_2, H_2, and H_2O. Formaldehyde and formic acid also decomposed via the surface formate. Thus the decomposition of methanol and formaldehyde was accompanied by surface reduction. No coverage dependence of product distribution was observed. On the Zn polar (0001) surface, methanol decomposed in two competitive pathways via a common formaldehyde intermediate. In one pathway, dehydrogenation of formaldehyde to CO occurred. In the other pathway, oxidation by lattice oxygen to a formate intermediate occurred which eventually decomposed into CO, CO_2, H_2, and H_2O above 400°C. The competition between dehydrogenation and oxidation depended on the coverage such that dehydrogenation was more favored for higher coverages. Within the dehydrogenation pathway, the selectivity for formaldehyde versus CO was lower for higher coverages. Within the oxidation pathway, the selectivity for CO versus CO_2 increased with higher coverages. Formaldehyde and formic acid also decomposed via the formate intermediate. The desorption of all decomposition products was reaction-limited except for water which was desorption-limited. The results indicated that the (0001) surface is more metallic in its behavior than the ($10\bar{1}0$) and ($50\bar{5}1$) surfaces. Comparison of the desorption temperatures of different compounds suggests that at room temperature, alcohols adsorb molecularly on the (0001) surface, but dissociatively on the other two surfaces. On the (0001), comparison among methanol, ethanol, and isopropanol suggests that the ease of dehydrogenation parallels the strength of the $\alpha_{C\text{-}H}$ bond.

INTRODUCTION

The chemical properties of single crystal metallic surfaces have been extensively investigated in the past 15 years (*1*). It is found that in many instances, different crystal faces exhibit different properties. Similar studies on oxide single crystal surfaces have been primarily limited to $SrTiO_3$, TiO_2, and ZnO (*2, 3*). We have recently employed temperature-programmed desorption and reaction to study the adsorption and desorption of CO, CO_2, O_2, and methanol from the nonpolar ($10\bar{1}0$), the stepped ($40\bar{4}1$) and ($50\bar{5}1$), and the Zn polar (0001) surfaces of ZnO (*3–5*) (Fig. 1). The behavior of the stepped surfaces in CO and CO_2 desorption is interesting in that they behave like the flat nonpolar surface in CO_2 desorption, but like the Zn polar surface in CO desorption. Desorption of methanol is accompanied by decomposition. On the ($10\bar{1}0$), ($40\bar{4}1$), and ($50\bar{5}1$) surfaces, the decomposition products are methane, CO, CO_2, and H_2. On the (0001) surface, the products are formaldehyde, CO, CO_2, H_2, and H_2O (*5*). Furthermore, it was found that within experimental uncertainties, the

[1] To whom correspondence should be addressed.

0021-9517/84 $3.00

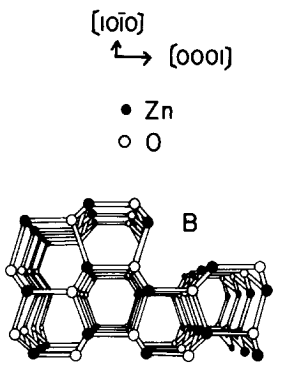

FIG. 1. Schematic representation of the different ZnO surfaces. The top surface is a stepped (n o $\bar{n}$ 1) surface. The top surface without the step would be a (10$\bar{1}$0) surface. The vertical surface on the right is the (0001) surface.

ratios of the decomposition products are the same on the (10$\bar{1}$0) and the stepped surfaces. However, the fraction of desorption products being decomposition products is higher on the surface with a higher step density, and is very small on a stoichiometric (10$\bar{1}$0) surface (*4, 5*). From this, it was concluded that the presence of defects is important for the decomposition activity.

We report here the results of the study on the mechanism of the methanol decomposition reaction on these surfaces. The mechanism is deduced from comparison among the decomposition reactions of methanol, formaldehyde, and formic acid. Hopefully, understanding the methanol decomposition reaction would shed light on the methanol synthesis reaction since they are related by the principle of microscopic reversibility.

Since the behavior of the stepped (50$\bar{5}$1) and the nonpolar (10$\bar{1}$0) surfaces in these reactions is very similar except for the decomposition activity, it is reasonable to assume that the reaction mechanisms are identical on these surfaces. Thus most of the studies were performed on the (50$\bar{5}$1) and the (0001) surfaces. Results from these surfaces will be compared. From these results and other relevant results from other studies, a conclusion regarding the variation in chemical properties of the different surfaces will be presented.

The (50$\bar{5}$1) and the (10$\bar{1}$0) surfaces will be collectively referred to as the nonpolar surface unless distinction is necessary.

EXPERIMENTAL

Experiments were conducted in a conventional ultrahigh vacuum chamber equipped with Auger and LEED optics and a UTI quadrupole mass spectrometer as described before (*3–5*). Zinc oxide single crystals were insulating samples purchased from Atomergic Chemicals. They were first aligned by X-ray Laue backscattering and then mechanically polished. The direction of the *c*-axis was determined by etching. The back and the edge of the samples were covered with gold by sputter deposition. The crystal faces being studied were about 6×6 mm^2. The surfaces were cleaned and annealed by repeated cycles of sputtering and annealing. The (10$\bar{1}$0) and the (0001) surface were annealed at 500°C for 60 min each time, and the (50$\bar{5}$1) surface was annealed first at 650°C for 30 min, and then at 500°C for 20 min. Details of the preparation have been reported (*3, 4*).

As reported before (*3, 4*), the LEED patterns of these surfaces showed a 1×1 pattern for (10$\bar{1}$0), a 1×1 pattern with split spots for (50$\bar{5}$1), and a sixfold "1×1" pattern with no discernable splitting of spots for (0001). Auger spectroscopy showed clean surfaces of (10$\bar{1}$0) and (50$\bar{5}$1). For the (0001) face, trace amounts of C, S, and Cl, but no K, were detected. Temperature-programmed decomposition (TPD) results from this surface compared well with those of another (0001) surface from another sample which showed the presence of K impurity but nothing else (*5*). After the initial cleaning and ordering, reproducible results were obtained from the nonpolar surfaces immediately. For the (0001) surface, about 3 or 4 experiments had to be performed before reproducible TPD results were obtained. However, LEED or Auger analysis did not indicate any observable changes except perhaps for a slight increase in the LEED background intensity. Reproducible

results were obtained immediately after subsequent sputtering and annealing.

The crystals were heated at the back by radiation from a tungsten filament. The temperature was measured with a thermocouple pressed by its own tension onto the front face of the crystal. Although this method does not guarantee that the correct temperature is read, it was found that the temperature-programmed decomposition (TPD) peak temperatures were reproducible on the $(10\bar{1}0)$ and the (0001) surface from sample to sample, and on the same sample among different mountings. On the $(50\bar{5}1)$ surface, however, the temperature reading seemed to be more sensitive to the thermocouple position. In the earlier experiments, shifts in TPD peaks from one thermocouple mounting to another was observed although the order of the peaks and their areas were independent of the shift. This problem of peak position shift was later solved by critical positioning of the thermocouple.

CD_3OD, CH_3OD, D_2CO, and DCOOD were purchased from Merck. They were +98 or +99% pure in the deuterium content. They were purified by vacuum distillation a few times, followed by several freeze–thaw cycles. Adsorption was achieved by dosing the desired compound directly onto the sample surface via a stainless-steel doser as described before (*4*, *5*). During dosing, the background pressure typically increased to 1 to 2 $\times$ 10^{-9} Torr (1 Torr = 133.3 Pa). The effective pressure at the surface was probably 10 to 100 times higher. The desorption characteristics of the surfaces studied did not depend on whether or not the nude ion gauge was turned on during adsorption.

Adsorption was achieved at room temperature. A typical exposure was for 20 s. In runs using different coverages, the exposure varied from 0.1 $\times$ 10^{-9} Torr (background pressure) for 2 s to 5 $\times$ 10^{-9} Torr for 20 s. After adsorption, the chamber was evacuated for 2 min during which the filament of the mass spectrometer was momentarily flashed to get rid of adsorbates on the filament. Desorption was then performed with the sample facing the mass spectrometer. The heating rate was 10°C s^{-1} up to 550°C at which temperature the sample was held for about 1.5 min. This procedure resulted in complete desorption of all surface species as determined by Auger spectroscopy. Even after weeks of experimentation, no detectable increases in C, S, or K (the typical impurities) were observed. There were no desorption peaks beyond 550°C (up to 600°C). Cooling from 550°C to room temperature took about 1 h. If a blank desorption was performed after this, the only major peak observed was that of water which will be described later.

The cracking patterns of the samples used were obtained by scanning the mass spectrometer from m/e = 1 to 70. These patterns are shown in Table 1. They were used for analysis of the TPD results and to show the absence of impurities in the samples. However, it was found that there was hydroxyl exchange taking place at the detector of the mass spectrometer. For example, the gas phase cracking patterns of CD_3OD, CH_3OD, and DCOOD also showed cracking patterns of CD_3OH, CH_3OH, and DCOOH, respectively. That the detection of OH compounds was due to hydroxyl exchange at the mass spectrometer was confirmed by a combination of several observations. Analysis of the liquid samples of CD_3OD and CH_3OD with proton NMR did not detect any OH species. The amount of exchange was not affected by baking out the gas-handling manifold outside the vacuum chamber or the vacuum chamber itself, but was affected by the time the mass spectrometer filament was turned on. It also depended on the nature of the previous experiments. Finally, the absence of such exchange for CD_2O and CD_4, and the exchange of protonated compounds (CH_3OH, HCOOH, H_2O) into OD compounds also supported the assignment. Such hydroxyl exchange has been reported by others (*6*).

TABLE 1

Cracking Patterns

Compounds	*m/e*																											
	2	3	4	12	13	14	15	16	17	18	19	20	28	29	30	31	32	33	34	35	36	40	43	44	45	46	47	48
DCOOD				5.1		4	2.3	10.2	7.95	20.5	17.6	10.8	45.5	11.93[a]	100								1.3	28.4	13[a]	27.8	31.2[a]	21.6
DCOOD[b]				5.1		4	2.3	10.2	7.95	20.5	17.6	10.8	45.5	11.93[a]	100								1.3	28.4	40.8		52.8	
HCOOH				4	1.9	1.9	6	10	21	76	1	4	53	100	4	6	4					1.5	6.5	43	43	53	1.2	
CD_3OD				3.8		6	2.4	15.5	2.4	75	2.4		14.3	10.7	100	4.76	8.3	95.2[a]	66.67	64.3[a]	40.5							
CD_3OD[b]				2.3		3.7	1.5	9.5	1.5	46.3	1.5		8.8	6.6	61.7	2.9	5	100		65								
CH_3OD				2.6	4.6	10.5	51	2.6	2.35	4.3	2		14.4	78.4	21.5	68[a]	100[c]	36										
CH_3OH				2.5	3.7	9.3	45.7	2.2	3.1	7.4	1.2	0.5	13.6	80.2	10	100	70.4	3.7										
CD_2O				4.1		5		6.4		0.9			34.5		100		75.5											
CH_2O[d]				3.3	4.3	4.4		1.7					30.9	100	88.5	1.9												
CD_4				3.28		10.25		14.75		75.4		100																
CH_4[d]				2.8	8.09	16.1	85.9	100	1.11																			
H_2O							1	3.5	26	100	10																	
CO_2				6				13		5		3	22											100	1.6			
CO[d]				4.7				1.7					100															
D_2	8.3	16	100																									
H_2	100	3																										
CD_3OD[d]				0.4		0.8		3		20			<7		27		5		100		83							
CH_3OD[d]				0.2	0.4	1.8	10						<3	18	6.8	5.1	100	79										
CH_3OH[d]				0.2	0.5	1.7	10.2						<4.8	33	5.2	100	80											

[a] The presence of these peaks is attributed to hydroxyl exchange in the mass spectrometer.
[b] The peaks with and without H—D exchange are summed together.
[c] Also includes the CH_3OH intensity due to exchange.
[d] Cracking patterns taken from literature Refs. (*6, 31, 32*).

As mentioned, the extent of hydroxyl exchange at the mass spectrometer varied with time. In the data reported, the peak intensities of the OD samples were corrected for the hydroxyl exchange using the best estimate of its extent at the time of the experiment. For example, in experiments using CD_3OD on the $(50\bar{5}1)$ surface, the amount of CD_3OD desorbed was measured as the area under the $m/e = 34$ (CD_2OD^+) peak multiplied by 200% to account for the fact that about 50% of the desorbed CD_3OD was detected as $m/e = 33$ (CD_2OH^+).

The peak areas reported in the tables are for data obtained with the sample facing the mass spectrometer. If the sample faced away from the mass spectrometer, the peak size typically was reduced from 50 to 70%, except for H_2 and D_2, which did not seem to decrease in size. Thus the mass spectrometer signals reported are not entirely due to direct flux from the sample. Since the behavior of all the peaks except H_2 and D_2 were similar, the relative amounts of the products were proportional to the relative peak areas after correction for the relative sensitivities.

The mass spectrometer sensitivities were determined for H_2, D_2, H_2O, CO, and CO_2 by leaking the appropriate gas individually into the chamber and measuring the corresponding mass spectrometer intensity. The pressure of the gas in the chamber was measured by an ion gauge. The introduction of one gas usually resulted in increase of the partial pressures of the other gases due to displacement. This effect was corrected for in the calculation of the partial pressure of the gas from the ion gauge reading, which was further corrected for the different ionization cross sections of different gases. The sensitivities were H_2, 7.2 A/Torr; D_2, 7.2, H_2O, 5.5; CO, 7; and CO_2, 5. From these, the relative sensitivities were calculated and were found to be similar to those obtained using the formula of Ko *et al.* (*7*), which gave H_2, 0.55; D_2, 0.66; H_2O, 1.2; CO, 1; and CO_2, 1.4.

If the ZnO sample was replaced by gold, no desorption peaks were detected using an otherwise identical procedure. Thus these results were not affected by desorption or reaction on places other than the sample.

RESULTS

As mentioned, the behavior of the nonpolar $(10\bar{1}0)$ surface and the stepped $(50\bar{5}1)$ surface in these reactions were similar except for the larger amount of decompositions from the $(50\bar{5}1)$ surface. Therefore, unless necessary, results from only the $(50\bar{5}1)$ and the (0001) surfaces are presented.

The TPD spectra was obtained by monitoring the relevant masses which represent various cracked fragments of various species. From these raw data and the cracking patterns of Table 1, the amounts of various species were determined. A sample of the raw data and a description of its treatment is presented in Appendix 1.

Results for the $(50\bar{5}1)$ Surface

Adsorption and desorption of water. The TPD profile of water adsorbed from the background is shown in Fig. 2a. A single peak at about 135°C was observed. It was not displaced by adsorption of methanol, formaldehyde, or formic acid. Its presence appeared to have no effect on the other molecules.

CH_3OD decomposition. A typical TPD profile of CH_3OD decomposition is shown in Fig. 3a. Two groups of products were observed. The group of peaks at 380°C was assigned to CO, CO_2, and H_2. Only H_2 was found to desorb. Table 2 lists the typical peak area ratios of these species. Because of a higher background for H_2, the uncertainty for this peak was much larger than that for CO, which was larger than that for CO_2. This is reflected in a much larger variation in the H_2 area than in other species. The situation was improved for other adsorbates of higher coverages which yielded larger signals. Finally, the noise level in the data made the detection of small amounts of water impossible.

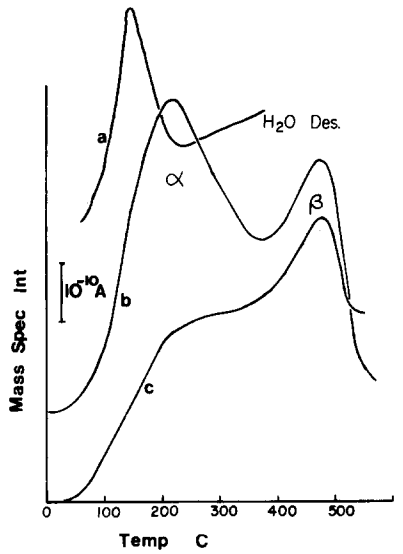

FIG. 2. Desorption spectra of water. Curve a: background adsorption on a (50$\bar{5}$1) surface; curve b: saturation coverage on a (0001) surface; curve c: background adsorption on a (0001) surface.

The group of peaks at about 150°C were assigned to undecomposed CH_3OD and methane. A water peak at 135°C that is not shown (see Appendix 1) was from adsorption of background water on cooling. The methane peak was a product of methanol decomposition. Its intensity did not correlate with the adsorbed background water intensity, suggesting that the latter does not affect the methane formation. As explained in the Appendix, the uncertainty in the *m/e* = 16 and 17 intensities did not permit quantitative determination of H/D isotope distribution in methane. Finally, we have looked for but did not find methyl formate, dimethyl ether, formaldehyde, and glycoaldehyde.

From the known pumping speed of the system and the mass spectrometer sensitivities, the surface coverage of methanol was estimated from the desorption peak areas to be about 1% of a monolayer (1 monolayer = 6×10^{14} molecules/cm^2).

To check whether methanol decomposition on the (50$\bar{5}$1) surface involved surface reduction, a series of CH_3OD decomposition was performed starting from a stoichiometric surface. The surface was made stoichiometric (*5*) by using a procedure based on the work of Göpel and co-workers (*8–10*) of annealing for 20 min at 400°C in 1 $\times$ 10^{-6} Torr O_2, cooled in O_2, and then flashed to 500°C to remove any adsorbed O_2. In each of these experiments, the methanol exposure was kept constant. After each desorption, the crystal was cooled to room temperature, exposed to methanol, and subjected to another desorption. The high temperature $CO_2/CO + CO_2$ peak ratios are plotted in Fig. 4, curve a, for each run. It was found to decrease with run num-

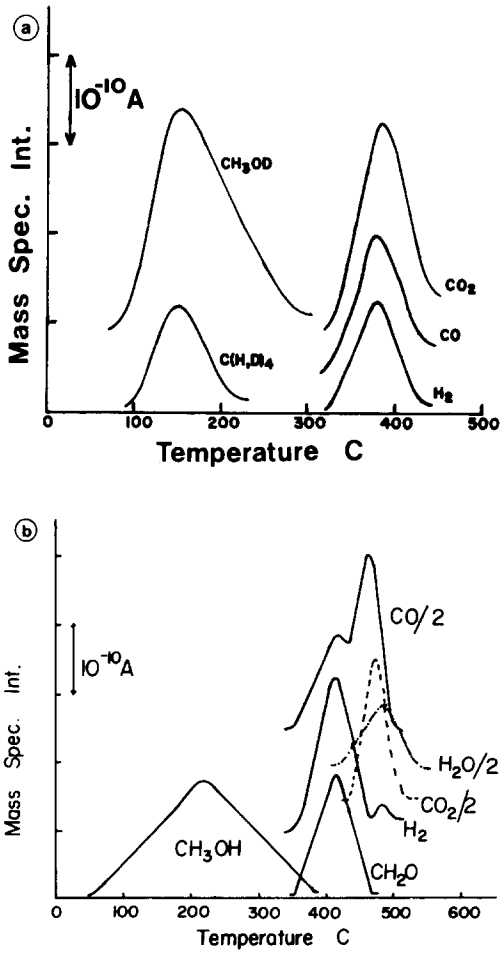

FIG. 3. TPD profile of methanol, temperature ramp 10 K s^{-1}. (a) CH_3OD from (50$\bar{5}$1) surface, the CH_3OD peak is the m/e = 32 peak. (b) CH_3OH from (0001) surface at saturation coverage.

TABLE 2

Peak Area Ratios of the High Temperature Decomposition Products from a $(50\bar{5}1)$ Surface.

Surface	Adsorbate	CO_2 area[a]	Relative areas[e]				
			$H_2(D_2)$[b]	CO	CO_2	$H_2O(D_2O)$[c]	Exposure[d]
$(50\bar{5}1)$	CH_3OH	2.64	0.83	0.66	1	0	$2/5 \times 10^{-9}$
		2.69	0.51	0.84	1	0	$5/3 \times 10^{-9}$
		3.9	1.38	0.76	1	0	$10/2.3 \times 10^{-9}$
	CH_3OD	3.2	0.38	0.49	1	0	[f]
$(10\bar{1}0)$	CH_3OD	9.37	[f]	0.53	1	0	$10/2 \times 10^{-9}$
		9.45	0.92	[f]	1	0	$10/2 \times 10^{-9}$
Average[g]	CH_3OH and CH_3OD		0.73 ±0.5	0.67 ±0.3	1	0	
$(50\bar{5}1)$	CD_2O	9.25	[f]	0.71	1	0.14	$10/.5 \times 10^{-9}$
		9.94	[f]	0.77	1	0.21	$10/1 \times 10^{-9}$
		8.27	[f]	0.64	1	0.17	$10/2 \times 10^{-9}$
		12.42	0.67	0.74	1	0.21	$5/8 \times 10^{-9}$
		11.77	0.68	[f]	1	0.21	$10/2 \times 10^{-9}$
		7.02	[f]	0.65	1	[f]	$10/2 \times 10^{-9}$
		6.66	[f]	0.51	1	0.18	$10/2 \times 10^{-9}$
Average[g]			0.63 ±0.20	0.73 ±0.06	1	0.19 ±0.04	
$(50\bar{5}1)$	DCOOD	88.0	0.48	0.73	1	0.22	$60/2 \times 10^{-9}$
		79.8	0.41	0.74	1	0.23	$30/2 \times 10^{-9}$
		38.9	0.38	0.77	1	0.20	$10/1 \times 10^{-9}$
		61.5	0.52	0.81	1	0.23	$20/2 \times 10^{-9}$
		55.7	0.46	0.77	1	0.23	$10/2 \times 10^{-9}$
Average[g]			0.47 ±0.41	0.78 ±0.09	1	0.22 ±0.04	

[a] The CO_2 areas are in arbitrary units.

[b] H_2 for compounds CH_3OH and CH_3OD, D_2 for CD_2O and DCOOD. H_2 was taken as the sum of the areas under $m/e = 2$ and 3, both of which were measured. D_2 was taken as $m/e = 4$, multiplied by 120% to account for H—D exchange at the mass spectrometer.

[c] H_2O for compounds CH_3OH and CH_3OD, D_2 for CD_2O and DCOOD. D_2O was taken as the area of $m/e = 20$, multiplied by 150% to account for H—D exchange at the mass spectrometer.

[d] Exposure is expressed as time (s)/background pressure (Torr).

[e] These areas are uncorrected for the relative mass spectrometer sensitivities.

[f] These values were not determined.

[g] These are average of more data than are shown.

ber, suggesting that the surface is being reduced.

If methanol was adsorbed at 230°C when the surface was free of adsorbed water, subsequent desorption yielded the same high temperature products. Thus the adsorbed background water had no effect on the decomposition reaction.

CD_2O decomposition. The product distribution in CD_2O decomposition on a $(50\bar{5}1)$ surface is shown in Fig. 5a. Undecomposed CD_2O desorbed at 130°C. At 380°C the decomposition products of CO, CO_2, D_2, and D_2O were desorbed. The amounts of these decomposition products are listed in Table 2. The peak areas were about four to five times larger than those from methanol.

The possibility that formaldehyde decomposition resulted in surface reduction was investigated in a similar manner as for methanol. Thus a stoichiometric surface was first prepared. Consecutive desorption of CD_2O was then performed. The variation of the $CO_2/(CO + CO_2)$ peak area ratio with

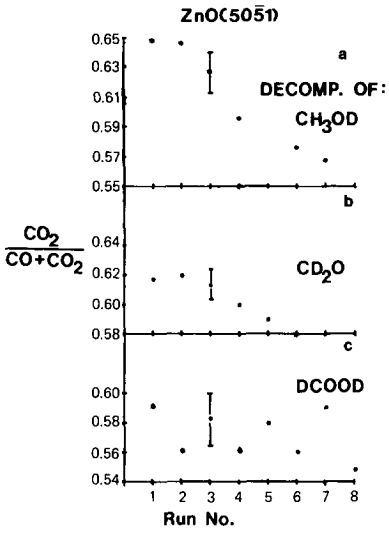

FIG. 4. The peak area ratio of $CO_2/(CO + CO_2)$ as a function of the number of consecutive TPD runs on a (50$\bar{5}$1) surface. Curve a: CH_3OD decomposition; curve b: CD_2O decomposition (average of three experiments); curve c: DCOOD decomposition. Exposures were 10 s at 2×10^{-9} Torr.

run number is shown in Fig. 4, curve b. Each data point represents the average of three experiments. The ratios were found to decline with increasing run number. Some other ratios, such as D_2O/CO, CO_2/CO, and O/C (measured as $(2CO_2 + D_2O)/(CO + CO_2)$) also declined with run number. However, the D_2O/CO_2 and $D_2O/(CO + CO_2)$ ratios declined from the first to the second run and then became constant afterward.

DCOOD and HCOOH decomposition. The product distribution in DCOOD decomposition on a (50$\bar{5}$1) surface is shown in Fig. 6a. No undecomposed formic acid desorbed. The decomposition products of CO_2, CO, D_2, and D_2O desorbed simultaneously at 380°C. The following species were looked for but not found: methyl formate, formaldehyde, methanol, methane, dimethyl ether, and glycoaldehyde. The ratios of the various products are listed in Table 2. Using HCOOH, the decomposition was studied on both a (10$\bar{1}$0) and a (50$\bar{5}$1) surface. The decomposition products and temperatures were the same on both surfaces, and very similar to DCOOD decomposition. The amount of decomposition products from a (50$\bar{5}$1) surface were about twice that from a (10$\bar{1}$0) surface.

The possibility that formic acid decomposition resulted in surface reduction was investigated in a manner similar to that used for formaldehyde and methanol. Thus consecutive desorption was performed starting with a stoichiometric surface and the resulting $CO_2/CO + CO_2$ ratios are shown in Fig. 4, curve c. Unlike the data for methanol and formaldehyde, these ratios did not show a systematic decrease with run number. Similar conclusions could be drawn for other ratios.

A summary of the peak ratios of the de-

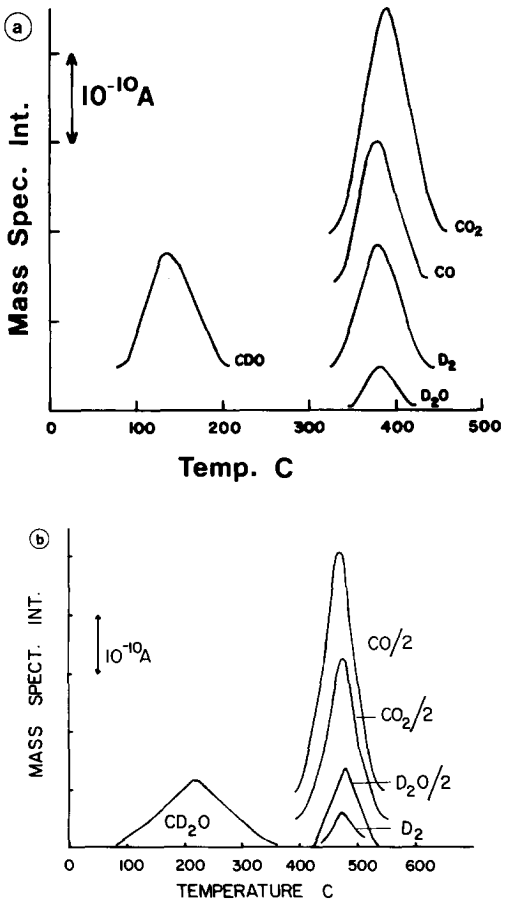

FIG. 5. TPD profile of CD_2O. (a) (50$\bar{5}$1) surface; (b) (0001) surface at saturation coverage.

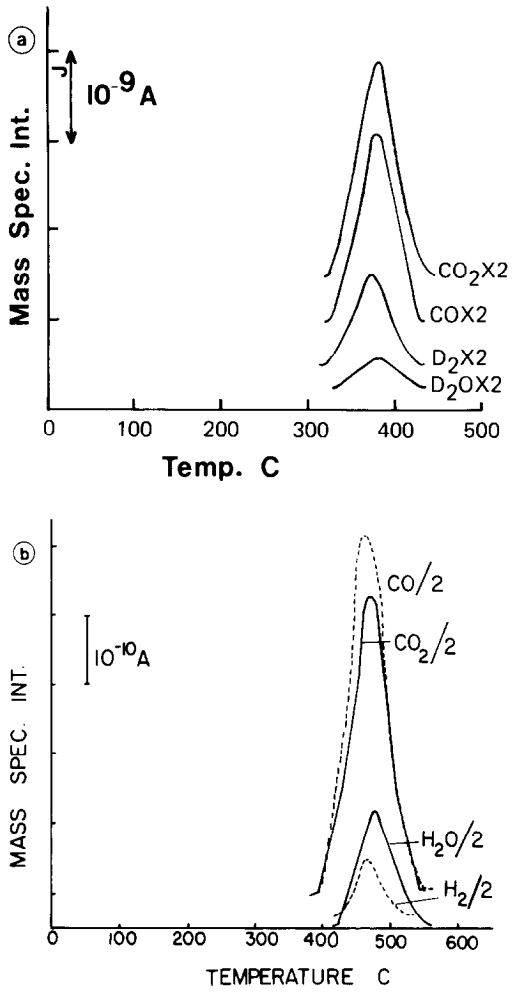

FIG. 6. TPD profile of formic acid: (a) DCOOD on a (50$\bar{5}$1) surface; (b) HCOOH on a (0001) surface at saturation coverage.

composition products for formic acid, formaldehyde, and methanol are shown in Table 2.

Coverage dependence of product distribution. Because of the low coverages involved in these experiments, the coverage dependence was investigated only over a limited range. As can be seen from the typical data shown in Table 2, there does not appear to be a strong coverage dependence for any of the three compounds studied.

Results for the (0001) Surface

Adsorption and desorption of water. Figure 2 shows the desorption spectra of water. Two desorption peaks, α and β were observed. A comparison between curve b for a saturation coverage and curve c for background adsorption shows that intentional exposure of the surface to water resulted in a much larger desorption peak α and a somewhat larger peak β. The temperature at peak maximum of the α peak decreased with increasing coverage from 280°C initially to 230°C at half saturation, and then stayed at 230° until saturation. Within experimental error (±5°C), the temperature at peak maximum of the β peak did not show coverage dependence. The β state was found to be completely displaced by the adsorption of CD_3OD, CD_2O, and DCOOD. The α state was also completely displaced by the adsorption of formic acid. Whether it is also displaced by CD_2O and CD_3OD is not known because these two compounds are also desorbed at about 220°C and their cracked fragments interfered with the detection of a small α water peak.

CH_3OD, CD_3OD, CH_3OH decomposition. The TPD spectrum of CH_3OH for a saturation coverage is shown in Fig. 3b. Undecomposed methanol was desorbed at about 220°C. At 410°C, formaldehyde, H_2, and CO were desorbed. The last group of products, CO, H_2, CO_2, and H_2O were desorbed between 460 and 490°C.

When CH_3OD was used instead of CH_3OH, the undecomposed methanol was entirely CH_3OD, and the hydrogen peak at 410°C was entirely H_2. The m/e = 3 (HD) peak at that temperature was less than 4% of the m/e = 2 peak, and it could be accounted for by H—D exchange at the mass spectrometer (see Table 1). For the water peak at 480°C, the m/e = 18/19 ratio was about 2.5 which was the ratio expected for H_2O counting H—D exchange at the mass spectrometer. Thus there was no deuterium in the decomposition products detected except the undecomposed CH_3OD.

When CD_3OD was used, the hydrogen peak at 410°C was D_2 (m/e = 4). No HD

was detected. For the water peak at 480°C, the ratio of m/e = 20 to 19 peaks was about 2.5, which was consistent with pure D_2O after correction for H—D exchange at the mass spectrometer. Within experimental error (±5°C) the peak temperatures were the same using CD_3OD and CH_3OH.

The coverage dependence of the decomposition product distribution is shown in Figs. 7–9. The relative areas of the CH_2O and the CO (410°C) peaks changed with surface coverage (Fig. 7). At low coverages CH_2O was a much more prominent product than CO. The two products became equally prominent at high coverages. The ratio of the high temperature CO and CO_2 peaks (470°C) also varied with coverages as shown in Fig. 8. The CO/CO_2 ratio was found to increase with increasing coverage. Figure 9 shows the variation with coverage in the production of CH_2O and CO (410°C) versus the higher temperature CO and CO_2. The selectivity for CH_2O and CO (410°C) increased with increasing coverages.

The temperatures at peak maximum for the products formaldehyde, CO (410°C), and H_2 (410°C) decreased from 435°C at low coverage to 410°C at saturation. The peak temperatures of the undecomposed methanol, H_2O (480°C), CO (470°C), and CO_2 (470°C) either decreased slightly (less than 10°C) or were constant with increasing coverage.

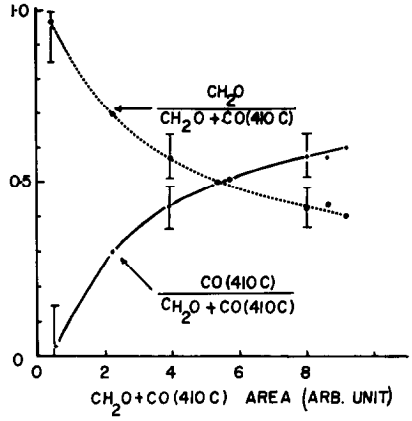

FIG. 7. Coverage dependence of the relative amounts of the CH_2O and the CO (410°C) peak in methanol decomposition on a (0001) surface. These areas have not been corrected for mass spectrometer sensitivities.

The effect of surface reduction on methanol decomposition was investigated by performing successive TPD of CD_3OD starting with a (0001) surface that was given an identical treatment that would result in a stoichiometric (10$\bar{1}$0) surface. The product

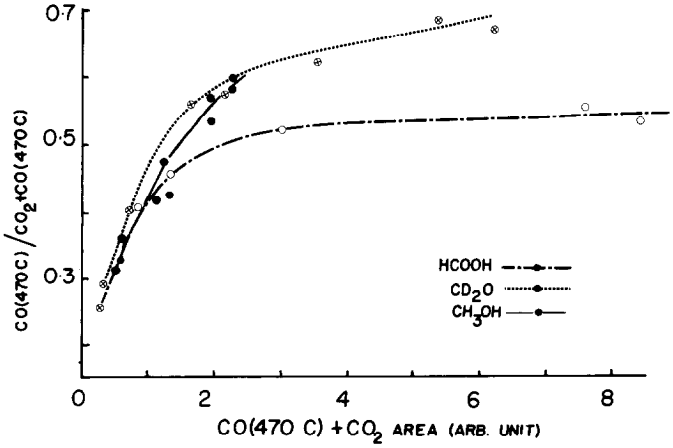

FIG. 8. Coverage dependence of the ratio CO/(CO + CO_2) in the high temperature (470°C) products in the decomposition of methanol, formaldehyde, and formic acid on a (0001) surface. The x-axis is the sum of the CO (470°C) and CO_2 (470°C) areas. The areas have not been corrected for mass spectrometer sensitivities.

ratios, D_2O/CO (470°C), and CO_2 (470°C)/[CO_2 (470°C) + CO (470°C) + CO (410°C)] for saturation coverage were plotted in Fig. 10 for the various runs. The former ratio was found not to change, but the latter ratio decreased with run number. The ratio CO_2 (470°C)/[CO_2 (470°C) + CO (470°C)] also decreased with run number. The decrease in these ratios suggested that the ZnO (0001) surface was reduced in the decomposition reaction.

Finally, some other possible products were searched for but not found. They included methane, acetone, dimethylether, and methyl formate.

CD_2O decomposition. The product distribution in the TPD of CD_2O at saturation coverage is shown in Fig. 5b. Undecomposed formaldehyde was desorbed at about 220°C. CO, CO_2, and D_2 were desorbed at about 470°C, and D_2O at 480°C. No HDO beyond that due to H—D exchange of D_2O at the mass spectrometer, and no H_2O were detected.

The product distribution depended on the coverage in a manner similar to methanol decomposition, as is shown in Fig. 8. The CO/CO_2 ratio was found to increase with higher coverages. The different coverages were calculated from the desorption peak areas for experiments using different exposures, ranging from 2 s at 0.1×10^{-9} Torr (nominal) to 20 s at 1×10^{-9} Torr (nominal). Table 3 shows the corresponding ratio of D_2O (sum of D_2O and HDO) to CO + CO_2.

Methane, oxygen, acetone, dimethyl

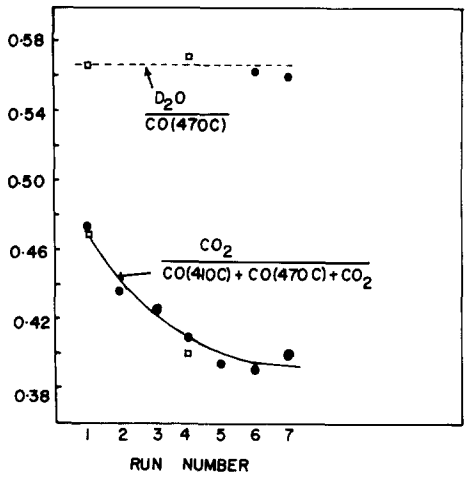

FIG. 10. Variation in the ratio D_2O/CO (470°C), and CO_2 (470°C)/C, where C = CO_2 (470°C) + CO (470°C) + CO (410°C), with run number for CD_3OD decomposition on a (0001) surface. The filled data points are for the first series of experiments, the empty points are for the second series.

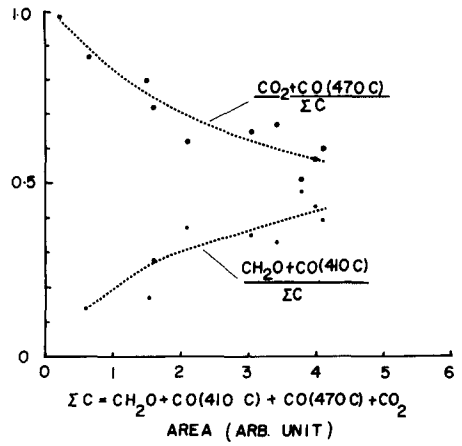

FIG. 9. Coverage dependence of the production of CH_2O and CO (410°C) versus the CO (470°C) and CO_2 (470°C) in the decomposition of CH_3OH on a (0001) surface.

TABLE 3

Variation of product distribution in CD_2O decomposition on a (0001) surface with exposure.

Exposure[a]	$D_2O/(CO + CO_2)$[b]	D/C[c]	O/C[c]
$2/0.1 \times 10^{-9}$	0.14	0.28	1.8
$5/0.1 \times 10^{-9}$	0.16	0.32	1.68
$5/0.2 \times 10^{-9}$	0.13	0.26	1.64
$5/0.4 \times 10^{-9}$	0.18	0.38	1.65
$3/1 \times 10^{-9}$	0.17	0.36	1.57
$20/1 \times 10^{-9}$	0.17	0.36	1.59

[a] Exposures are expressed in time (s)/pressure (Torr).

[b] The value for D_2O is the sum of HDO and D_2O. These ratios are ratios of mass spectrometer peak areas after correction for the cracking patterns.

[c] D/C is $2(D_2 + D_2O)/(CO + CO_2)$. O/C is $(CO + 2CO_2)/(CO + CO_2)$. These ratios have been corrected for the cracking patterns and the mass spectrometer sensitivities.

ether, methyl formate, and methanol were looked for but not found as products.

HCOOH, HCOOD, and DCOOD decomposition. The product distribution at saturation coverage is shown in Fig. 6b for HCOOH decomposition. It can be seen that there was no desorption below 400 C—no α state of the background water, and no undecomposed formic acid. The decomposed products of CO, CO_2, and H_2 were desorbed at 460–470°C, and H_2O at 480°C. Using DCOOD instead of HCOOH, the H_2O peak became D_2O entirely, and the H_2 became D_2. The CO and CO_2 peaks remained unchanged. There was no detectable shifts in peak temperatures either. On the other hand, the decomposition products for HCOOD were identical to those for HCOOH, that is, no deuterium-containing compounds were detected.

The displacement of the α-state water by formic acid was confirmed by first exposing the surface to water to populate the α state, then to formic acid. Upon desorption, no water peak at 230°C was found.

The coverage dependence of the decomposition products is shown in Fig. 8. Similar to formaldehyde and methanol decompositions, the selectivity for CO versus CO_2 increased with increasing coverage.

The species that were searched for but not found included methane, methanol, acetone, dimethyl ether, and methyl formate.

DISCUSSION

The discussion will be in five parts. First, the decomposition of methanol, formaldehyde and formic acid on the nonpolar surfaces will be compared. Second, their decomposition on the Zn polar surface will be compared. Third, the similarities and differences between the nonpolar and the polar surfaces will be discussed. This is followed by the mechanism of methanol decomposition on these surfaces. Finally, the general properties of these surfaces derived from the present study will be presented.

Reaction on the ($10\bar{1}0$) and the ($50\bar{5}1$) surfaces. The decomposition of methanol, formaldehyde, and formic acid on these surfaces show some interesting differences and similarities. Two and possibly three differences were observed. First, methane is produced from methanol but not from formaldehyde or formic acid. Second, both methanol and formaldehyde decomposition result in a reduction of the surface as evidenced by a change in the CO_2/CO ratio in the products in consecutive experiments starting from a stoichiometric surface. On the other hand, formic acid decomposition does not result in surface reduction. A third difference, that water was detected as a product for formaldehyde and formic acid but not for methanol, may not be real. This is because water may be formed in methanol decomposition, but the low coverage of methanol made it undetectable.

The production of methane is also a difference between the nonpolar and the polar surfaces. Thus this point will be discussed in that section.

The reduction of the surface by methanol and formaldehyde must be associated with the formation of the high temperature products. Since formic acid does not result in surface reduction, it suggests that in the formation of the high temperature products, both methanol and formaldehyde are first oxidized to a formate-like species which is then decomposed. This proposal is further substantiated by the similarities among the decomposition of the three compounds.

Two important similarities were observed in the decomposition reactions. First, the decomposition products were all evolved at the same temperature of 380°C. Second, the ratios of the products were similar (Table 2), especially the CO_2/CO ratio. The D_2O/CO_2 ratios were also similar, but the uncertainties were larger. For the ratios of H_2 (or D_2)/CO_2, there might be a trend of increasing H_2 desorption going from formic acid, to formaldehyde, and to methanol.

These similarities strongly suggest that the precursor intermediate leading to the

formation of CO, CO_2, $H_2(D_2)$, and $H_2O(D_2O)$ is the same for the three compounds studied. That these products were evolved at the same temperature which is higher than when the gases were adsorbed alone (*3, 4*) suggests that their desorption was reaction limited.

A likely precursor is a formate or a formate-like intermediate such as one involving a strong interaction between adsorbed formate and adsorbed CO. A formate precursor has been proposed in the decomposition of formic acid on many metal surfaces and oxygen-covered metal surfaces. In most cases, however, CO_2 and H_2 were the decomposition products. On Ru(001) and Ni(110), CO, CO_2, H_2, and H_2O were formed, and that formate was the precursor was confirmed by high-resolution electron energy loss spectroscopy (*11, 12*). On Fe (100), CO, CO_2, H_2, and adsorbed oxygen were the products, and the formate precursor was inferred from stoichiometry measurements (*13*). Formate and its derivatives have been proposed in formic acid decomposition on Ni(110) (*14*), Ni(100) (*15*), Ru(1010) (*16*), and Ni(110) (2 × 1)O (*17*). CO, CO_2, H_2, and H_2O were the products.

On ZnO powders, infrared studies by Ueno *et al.* (*18*) and TPD studies by Bowker *et al.* (*19*) have indicated the presence of formate species in methanol decomposition. The same infrared spectrum was observed by Noto *et al.* on adsorption of formic acid (*20*). In view of these data, the decomposition intermediate in our experiments is likely a formate or formate-like species.

Reactions on the Zn polar surface. Water is adsorbed on this surface in two states. The higher temperature β state was completely displaced by adsorbed formic acid, formaldehyde, and methanol. The lower temperature α state was also displaced by adsorbed formic acid. While similar data were not available for formaldehyde and methanol, the fact that these two compounds displace the β state suggests that they would most likely displace the α state which binds less strongly than the β state. The displacement of the β state by methanol appears to be molecule for molecule. It was found that as the coverage of CD_3OD decreased, the β-state background water peak (H_2O) increased, while the decomposition product D_2O decreased proportionally.

Methanol decomposes into two sets of products: one at 410°C which consists of formaldehyde, hydrogen, and CO; the other at 470–480°C which consists of CO, CO_2, H_2O, and a small amount of H_2. The higher temperature set of products appeared to be identical for methanol, formaldehyde, and formic acid. They were desorbed at identical temperatures, and the ratios of CO/CO_2 (Fig. 8) and H/C were the same within experimental uncertainties for the three compounds. The desorption of this set of products, except H_2O at 480°C is reaction-limited because the products were evolved at the same temperature, and, if the products were adsorbed individually, they would desorb at lower temperatures (*3*). The desorption of water, however, is desorption-limited.

The identical ratios of the decomposition products at 470–480°C even for different coverages strongly suggest that the precursor intermediate is a formate-like species. In the formation of the formate intermediate from methanol, the ZnO surface must be reduced. This is reflected in the decreasing CO_2/CO ratio with increasing run number in a series of successive methanol decomposition experiments (Fig. 10). Direct evidence of formate can be provided by vibrational spectroscopy which has to be performed. As mentioned before, the existence of formate has been confirmed on ZnO adsorption of formic acid (*20*), and from temperature programmed decomposition experiments (*19*). The proposal of a formate intermediate in formic acid decomposition is common on metal surfaces (*11–13*).

Ueno *et al.* (*18*) produced formate on ZnO powders by coadsorption of CO_2 and

H_2 at 230°C. On decomposing the formate at the same temperature, they found that the selectivity for CO decreased with increasing coverage, which is opposite to what was observed in this study (Fig. 8). One possible explanation is that the decomposition in their experiments was at 230°C, but was at about 450°C in our experiment. We have performed an experiment in which formic acid was adsorbed at 230°C. Subsequently TPD yielded the same product as room temperature adsorption. On the other hand, we observed that on this (0001) surface, adsorption of CO_2 at elevated temperatures resulted in a production of CO and adsorbed oxygen on subsequent TPD, in addition to CO_2 desorption. The yield of CO was maximum when CO_2 was adsorbed at about 230°C. It decreased with increasing coverage of adsorbed oxygen on the surface. If this CO_2 decomposition reaction contributed in their experiment, it could account for the decrease in CO yield with increasing coverage of formate.

The decreasing CO_2/CO ratio with increasing coverage may indicate the increased tendency for the formation of formic anhydride:

$$2HCOO\ (a) \rightarrow HC(=O)OC(=O)H(a) + O\ (a)$$

Increasing the surface coverage of formate should drive the reaction to the right. The CO_2/CO ratio is expected to be higher for the formate than for the formic anhydride. The proposal that the latter is an intermediate in formic acid decomposition is also common on metal surface (*15–17*). The O(a) is readily reduced by H_2 generated in the decomposition to form H_2O. This could explain the constant $D_2O/(CO + CO_2)$ ratio independent of coverage observed in CD_2O decomposition (Table 3). That O(a) can be reduced by $H_2(g)$ has been confirmed in this laboratory.

In the decomposition of methanol, there is an additional pathway that leads to the production of CH_2O, CO, and H_2 at 410°C. The nature of the products suggests that the pathway involves dehydrogenation and is probably totally independent of the pathway of oxidation to form formate. Figure 9 shows that the selectivity for dehydrogenation increases with increasing coverage.

This change in selectivity can be explained by the fact that the oxidation pathway involves surface reduction, while dehydrogenation does not. With increasing coverage, the extent of surface reduction also increases in forming the formate, which makes this pathway less favorable compared to dehydrogenation. Within the dehydrogenation pathway, the yield of CO (410°C) relative to CH_2O increases with increasing coverage. This may indicate the fact that with increasing coverage, the surface is increasingly reduced due to increased formate formation. A more reduced surface is more metallic like. Since dehydrogenation to CO is a common reaction for methanol on metal surfaces (*21–24*), a more reduced surface would yield a higher CO/CH_2O ratio.

Comparison between the nonpolar and the Zn polar surfaces.

Comparison of these results obtained from the $(10\bar{1}0)$, $(50\bar{5}1)$, and (0001) surfaces shows more similarities and differences which reflect the different properties of the nonpolar and the polar surfaces. Several important differences can be identified. They include the behavior of adsorbed water, the product distribution in the decomposition reactions, the temperature of desorption of the products, and the coverage dependence of the product distribution.

Only one desorption peak for water at a relatively low temperature was observed on the nonpolar surfaces. Two peaks, one at a lower and one at a substantially higher temperature were observed on the (0001) surface. It is likely that the two peaks correspond to two modes of adsorption. One possibility is that the lower temperature peak is for the desorption of molecularly adsorbed water, and the higher temperature peak is for the desorption of dissociatively

adsorbed water. If water behaves like methanol, then following our proposed mechanism below, the single water desorption peak on the nonpolar surfaces would correspond to desorption of dissociatively adsorbed water. We shall return to this point later.

While the product distribution in formic acid and formaldehyde decompositions are roughly similar on all three surfaces, those for methanol decomposition differ significantly. In particular, methane is formed on the nonpolar surfaces, and the dehydrogenation reaction is more prominent on the Zn polar surface. There are two possible pathways for the production of methane on the nonpolar surface:

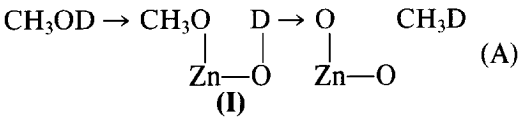

(A)

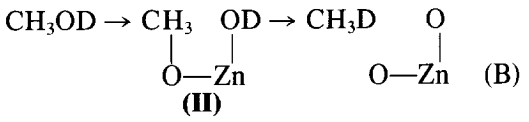

(B)

In these mechanisms, the methyl group remains intact and methane-d_1 would be the only methane product. Our data was not quantitative enough to permit determination of the isotope content of methane. However, the fact that only H_2 and no HD or D_2 was desorbed at 380°C from CH_3OD is consistent with the assumption that the methyl group was intact. In addition, in the infrared study of methanol adsorption on ZnO powder, a methoxy species was identified (*18*), suggesting that at least some of the methyl groups remain intact.

The overall mechanistic consequence of both path A and B is the same. Path B has been proposed for another basic oxide MgO (*25*), while path A has been proposed for an acidic oxide Al_2O_3 (*26*). Our data do not distinguish the two pathways. If all basic oxides behave the same, then path B would apply.

The absence of methane production on the (0001) surface may be due to either of the following reasons. Dissociative adsorption of methanol as in path A or B does not occur readily; or the O—CH_3 formed is so stable on this surface that the production of methane is no longer favorable; or the nature of the dissociatively adsorbed species are different on the different surfaces. For this last point, specifically, the dissociatively adsorbed methanol has the form of **I** or **II** in paths A or B on the nonpolar surfaces. It is expected that the dissociation would be more heterolytic. On the polar surface, a likely form is either III or IV, and the dissociation would be more homolytic.

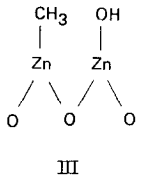

III

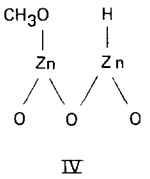

IV

The difference in their ionic character could result in different reactivities. Of these possibilities, the most likely one is the one that dissociative adsorption does not take place readily on the (0001) surface because of the large distance between the adjacent surface Zn ions and the rather weak Zn—CH_3 (or Zn—H) bond. Without the formation of **III** (or **IV**), methane is not formed. It is also for this reason that methanol adsorbs molecularly on the (0001) surface, and dissociative adsorption requires elevated temperature. On the nonpolar surfaces, dissociative adsorption readily occurs.

The production of formaldehyde and CO (410°C) on the (0001) surface suggests that dehydrogenation is more prominent on this surface. Since the dehydrogenation reaction is commonly observed on metals, this suggests that the (0001) surface is more metallic-like than the nonpolar surfaces. Indeed, the particular atomic arrangement of a zinc polar surface (in which a layer of Zn is more outwardly displaced than a layer of O) produces a strong dipole moment at the surface and a larger surface energy. To minimize both the dipole moment and the surface energy, the surface tends to recon-

struct, and the surface ions tend to carry a lower real ionic charge than the bulk ions. The lower real charge would make the ions on this surface more metallic in character than the ions on the nonpolar surfaces. On the other hand, the formation of formate from methoxy takes place at a lower temperature on the nonpolar surfaces. Thus the oxidation activity on the nonpolar surfaces is higher, which is consistent with the structure of the surface.

The coverages of the compounds studied, especially methanol, were much higher on the (0001) than on the nonpolar surfaces. This made possible the study of the coverage dependence of the decomposition products over a wide coverage, and a strong dependence was observed. The coverages on the nonpolar surfaces were low and, over the limited range of coverages studied, little variation was observed.

In spite of these differences, some interesting similarities were observed among the surfaces. The most striking similarity is the fact that the major decomposition pathways for methanol, formaldehyde, and formic acid appear to be the same. That is, they all proceed via the formate-like intermediate. The stability of this formate is slightly higher on the (0001) than on the nonpolar surfaces. Because the formate intermediate is involved, methanol decomposition reduces all the surfaces.

Proposed mechanisms. The mechanisms for methanol decomposition are summarized in Figs. 11 and 12 for the nonpolar and the polar surface, respectively. For the nonpolar surfaces, methanol is first adsorbed dissociatively both in paths A and B. At 150°C the methyl species in path B recombines with OD to desorb as CH_3OD, or combines with the D in OD to desorb as CH_3D. Some deuteron is desorbed on adsorption of methanol and is not detected. The remaining methoxy undergoes dehydrogenation to formaldehyde which is then rapidly oxidized by lattice oxygen to a formate-like species, which then decomposes to CO, CO_2, H_2O, and H_2 at 380°C.

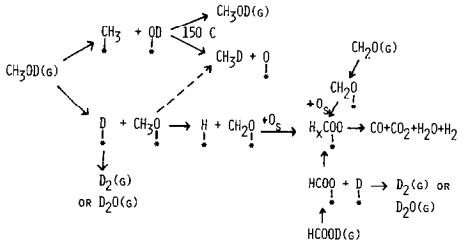

FIG. 11. Proposed reaction mechanism for the nonpolar surfaces.

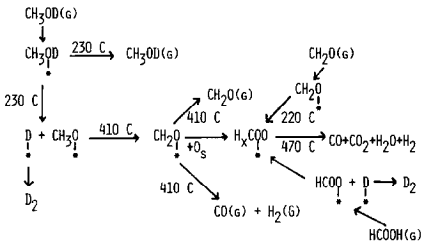

FIG. 12. Proposed reaction mechanism for the Zn polar surface.

Because of the low coverage of methanol and the fact that only about half of the adsorbed methanol decomposes (the rest is desorbed as methanol or forms methane), the mass spectrometer intensity for water is small and is not detected. Once the formaldehyde intermediate is formed, some of it may be desorbed. However, from results in formaldehyde decomposition, the fraction of formaldehyde desorbed is expected to be small and may not be detected. Alternatively, the dehydrogenation process occurs simultaneously with oxidation, and formaldehyde is not an intermediate of significantly long lifetime for detection.

The mechanism for formaldehyde decomposition follows the same pathway as methanol. Thus adsorbed formaldehyde, if not desorbed by 150°C is oxidized to the formate-like species by lattice oxygen. Similar mechanisms have been proposed for oxygen covered Ag (*27*) and Cu (*28*) surfaces.

Since lattice oxygen is involved in the formation of the formate-like species in these two reactions, the decomposition

product pattern is expected to depend on the reduction state of the surface. In particular the CO_2/CO ratio is expected to decrease on a more reduced surface as was observed.

The proposed formate-like intermediate is labeled $H_xCOO(a)$. It is used to indicate the ignorance in its hydrogen stoichiometry. It is possible that x is unity for formic acid decomposition, and is larger for formaldehyde and methanol.

Finally, it is interesting to note that undecomposed methanol and formaldehyde were detected desorbing at about 130 to 150°C, but no undecomposed formic acid was observed. Also, desorption of background water was present in all cases. Thus none of these compounds displaces adsorbed water, a case quite different from the zinc polar (0001) surface.

The proposed mechanism for the polar surface is summarized in Fig. 12. For methanol, it is first adsorbed molecularly. While our data do not strongly distinguish the possibility of molecular versus dissociative adsorption to form methoxide, the absence of methane product is more consistent with molecular adsorption. On heating to about 200°C, some of the methanol desorbs, while some undergoes dissociation to methoxide and hydrogen. On further heating to about 400°C, the methoxide undergoes dehydrogenation to formaldehyde. Then three competitive pathways occur. The formaldehyde can desorb. It can undergo further dehydrogenation to CO and H_2, and it can be oxidized by lattice oxygen to a formate-like intermediate. The competition among these three processes depends on the reductive state of the surface as was discussed earlier. The formate-like intermediate is denoted as $CH_xOO(a)$ in the figure to point out our ignorance in its hydrogen content. It also allows for a different hydrogen content for different coverages, and for different origins of its formation.

It is interesting to note that while adsorbed formaldehyde is postulated as an intermediate in methanol decomposition, formaldehyde TPD spectrum shows undecomposed formaldehyde at 225°C, no products at 410°C, and one set of products at 470–480°C. This suggests that oxidation of formaldehyde to formate takes place at about 225°C such that no dehydrogenation to CO is observed. This would imply that in methanol decomposition, the conversion of methoxide to formaldehyde is a rate limiting step. Once formaldehyde is formed at 410°C, its desorption, further dehydrogenation to CO, and oxidation to formate are all rapid and competitive.

The decomposition of formaldehyde and of formic acid proceed via the formate intermediate in the same manner as methanol.

From experiments using CH_3OD and HCOOD, it was found that the hydroxyl hydrogen was not observed in the decomposition products. In the case of formic acid, the D may have been desorbed as D_2 on dissociative adsorption of formic acid at room temperature, and was therefore not detected. For methanol, the dissociation of the O—D bond takes place at about 200°C. However, owing to the low coverage of methanol, and thus low concentration of the adsorbed D, the recombination of adsorbed D to form D_2 may be slow which would result in a broad D_2 peak not easily detectable.

Finally, for both nonpolar and polar surfaces, the peak intensities and positions were not affected by whether totally protonated reactants or totally deuterated reactants were used. This implies that the C—H and C—D bond breaking is not the rate limiting step, or that the transition state is very reactant-like that breaking of the C—H (C—D) bond has not taken place significantly. From our results, it is likely that in the decomposition of the surface formate, the breaking of C—O bonds is the rate limiting step for the oxidation pathway.

Comparison among different adsorbates. In addition to the similarities observed among formic acid, formaldehyde, and methanol decompositions, when these

results were compared with some other compounds, more interesting correlations can be found. Table 4 lists the peak temperatures of the desorption peaks of the undecomposed adsorbates. On the (0001) surface the temperatures are very similar. Formaldehyde and acetone do not possess hydroxyl hydrogen. Its adsorption must be molecular and, most likely, is via the oxygen interaction with the surface. Since, as we proposed, the alcohols also adsorb molecularly on this surface, the interaction would also be between the oxygen in the molecule and the surface. Therefore, it is not surprising that the desorption temperatures are similar. On the nonpolar surfaces, however, the desorption temperature for formaldehyde, acetaldehyde and acetone are somewhat lower than the alcohols. This may indicate that the modes of adsorption are different; namely, the alcohols are adsorbed dissociatively on these surfaces, and the aldehydes are adsorbed molecularly. Thus the alcohols are desorbed at a higher temperature.

Finally, there appears to be a correlation between the strength of the α C—H bond and the dehydrogenation activity as measured by the desorption temperature of the dehydrogenation products. Such a correlation is shown in Table 5. It can be seen that the stronger the α C—H bond, the higher is the temperature required. It suggests that for this dehydrogenation process, the breaking of the α C—H bond is involved in the rate limiting step. The absence of apparent difference between C—H and C—D bond is probably due to the smaller difference in their bond strengths than those among different hydrocarbons, such that the chemical shift is less than the noise of the experiment.

TABLE 4

Desorption Temperatures of Undecomposed Adsorbates on ZnO[a]

Adsorbate	Surface	
	$(10\bar{1}0),(50\bar{5}1)$	(0001)
H_2O	135 ± 5	230 ± 10[d]
CH_3OH	150 ± 5	220 ± 5
C_2H_5OH	130[b]	240 ± 5[c]
i-C_3H_7OH	150 ± 5[c]	240 ± 5[c]
CD_2O	125 ± 5	225 ± 5
CH_3CHO	105[b]	—
$(CH_3)_2CO$	105 ± 5[c,e]	250 ± 10[c]

[a] All temperatures are in degree centigrades for a heating rate of 10°C s^{-1} except for those indicated.
[b] Taken from Ref. (*29*). The heating rate was 11°C s^{-1}.
[c] Unpublished results from this laboratory.
[d] Temperature for saturation coverage. It is for the lower temperature peak.
[e] The lower temperature peak.

TABLE 5

Alkoxide Dehydrogenation Temperatures on a ZnO (0001) Surface

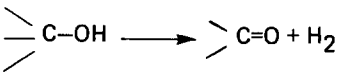

Alkoxide	Temperature[a] (°C)	α C—H bond strength[b] (kJ/mol)
CH_3O	410 ± 5	393 ± 7
C_2H_5O	375 ± 5[c]	389 ± 4
i-C_3H_7O	350 ± 5[c]	380 ± 4

[a] Temperature for a heating rate of 10 C sec^{-1}.
[b] Taken from Ref. (*30*).
[c] Unpublished results from this laboratory.

APPENDIX 1

Treatment of raw data to obtain TPD profiles. The raw data for CH_3OD on a $(50\bar{5}1)$ surface is shown in Fig. 1A. There were three groups of desorbed products. The lowest temperature group consisted of m/e = 18 and 19, with peak maximum at about 135 ± 5°C. The second group at a slightly higher temperature consisted primarily of m/e = 33, 32, 31, 17, and 16. The third group was at a distinctly higher temperature of about 380°C. The highest temperature products can be easily identified as CO_2, CO, and H_2 because their cracking patterns are distinct from each other (Table 1). The small m/e = 3 peak (HD) can be accounted for by hydroxyl exchange at the

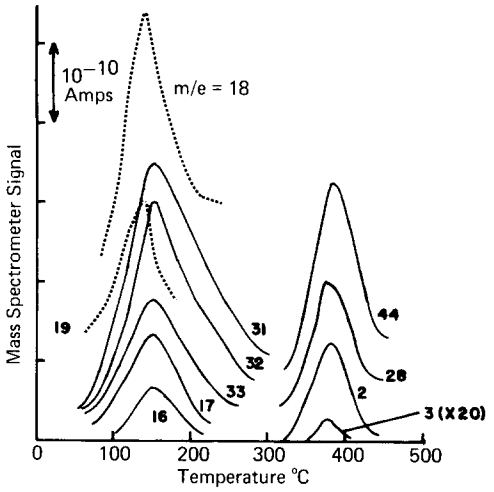

FIG. 1A. TPD profile of CH_3OD on a $(50\bar{5}1)$ surface showing the major mass spectrometer peaks.

mass spectrometer. No $m/e = 4$ peak was observed.

The $m/e = 18$ and 19 peaks were due to adsorption of background water as they were observed even in a blank desorption for a surface that underwent an identical pretreatment except without methanol adsorption (Fig. 2). The same $m/e = 18$ peak, at the same temperature and with at most a slight decrease in intensity, was observed. Furthermore this peak of about the same intensity was observed independent of whether CH_3OH, CH_3OD, CD_3OD, D_2CO, DCOOD, or HCOOH was adsorbed. The $m/e = 19$ peak observed in a blank desorption had a lower intensity of about 10% of the $m/e = 18$ peak as compared to about 30 to 50% in the desorption of any OD-containing compounds. We attribute this latter higher $m/e = 19$ intensity as primarily due to an increase in the extent of hydroxyl exchange at the mass spectrometer with minor, if any, contribution from H—D exchange on the sample surface because of the following reasons. When the chamber was dosed with CD_3OD and the gas phase H_2O cracking pattern was taken, the 19/18 peak ratio was about 20% compared to the normal 10% when no OD groups had been introduced previously. When DCOOD was adsorbed which had a much higher (about five times) coverage than methanol, the 19/18 peak ratio remained about the same. This suggested that no appreciable hydroxyl exchange on the surface took place. The 19/18 peak ratios for different adsorbates are shown in Table 1A. Clearly, the ratios were low and about the same for all OH-containing adsorbates, and high for all OD-containing adsorbates. While the evidence strongly suggested that the hydroxyl exchange was at the mass spectrometer, the possibility of a very small amount of exchange on the crystal surfaces cannot be excluded.

The $m/e = 33$, 32, and 31 peaks at 150°C were assigned to desorbed CH_3OD. The nearly equal intensities of these three peaks agreed with the cracking pattern in Table 1. Thus the $m/e = 31$ peak was due to hydroxyl exchange between CH_2OD^+ and some OH-containing species in the mass spectrometer, and not due to desorption of CH_3OH from the surface.

There were three contributions to the $m/e = 17$ and 16 peaks. One was from the cracking of CH_3OD. The second was from the cracking of the overlapping H_2O and HDO peaks. Both of these can be easily corrected with data of Table 1. However, these corrections introduced rather large uncertainties in the areas of these peaks.

TABLE 1A

Intensity Ratios of Mass 19 and 18 Peaks

Surface	Adsorbate	19/18 Area ratio
	Blank	0.10
$(10\bar{1}0)$	CH_3OH	0.11
	CH_3OH	0.07
	CH_3OD	0.41
	CH_3OD	0.47
	CH_3OD	0.50
	CD_3OD	0.45
$(50\bar{5}1)$	HCOOH	0.10
	CH_3OD	0.49
	CH_3OD	0.53
	DCOOD	0.64

These two peaks are attributed primarily to CH_3D and CH_4. The uncertainties in the data did not permit estimation of the relative amounts of the isotopic species. Therefore, whether the methyl group in methanol remained intact in the formation of methane has to be inferred from other data. While the isotopic content of methane was not certain, its identification was. First, the size of the m/e = 16 and 17 peaks could not be accounted for by cracking of methanol or water. Secondly, in the decomposition of CD_3OD, peaks of m/e = 20 (CD_4) and 18 (cracking of CD_4) were observed in place of 16 and 17. Similarly, in the decomposition of CH_3OH, peaks of m/e = 16 (CH_4) and 15 (cracking of CH_4) were observed instead.

After identifying the species that contributed to the various peaks, the TPD profile showing the relative amounts of various desorption products was constructed. Such a profile is shown in Fig. 3a.

ACKNOWLEDGMENT

This work was supported by the Division of Basic Energy Sciences, U.S. Department of Energy.

REFERENCES

1. Somorjai, G. A., "Chemistry in Two Dimensions: Surfaces." Cornell Univ. Press, Ithaca, N.Y., 1981.
2. Henrich, V. E., *Progr. Surf. Sci.* **9,** 143 (1979).
3. Cheng, W. H., and Kung, H. H., *Surf. Sci.* **122,** 21 (1982).
4. Cheng, W. H., Ph.D. thesis, Northwestern University, 1982.
5. Cheng, W. H., Akhter, S., and Kung, H. H., *J. Catal.* **82,** 341 (1983).
6. Beynon, J. H., Fontaine, A. E., and Lester, G. R., *Int. J. Mass Spectrom. Ion Phys.* **1,** 1 (1968).
7. Ko, E. I., Benziger, J. B., and Madix, R. J., *J. Catal.* **62,** 264 (1980).
8. Göpel, W., Brillson, L. J., and Brucker, C. F., *J. Vac. Sci. Technol.* **17,** 894 (1980).
9. Göpel, W., *Surf. Sci.* **62,** 165 (1977).
10. Runge, F., and Göpel, W., *Z. Phys. Chem. Neue Forge* **123,** 173 (1980).
11. Madix, R. J., Gland, J. L., Mitchell, G. E., and Sexton, B. A., *Surf. Sci.* **125,** 481 (1983).
12. Avery, N. R., Toby, B. H., Anton, A. B., and Weinberg, W. H., *Surf. Sci.* **122,** L574 (1982).
13. Benziger, J. B., and Madix, R. J., *J. Catal.* **65,** 49 (1980).
14. McCarty, J., Falconer, J. L., and Madix, R. J., *J. Catal.* **30,** 235 (1973).
15. Falconer, J. L., and Madix, R. J., *Surf. Sci.* **46,** 473 (1974).
16. Larson, L. A., and Dickinson, J. T., *Surf. Sci.* **84,** 17 (1979).
17. Johnson, S. W., and Madix, R. J., *Surf. Sci.* **66,** 189 (1977).
18. Ueno, A., Onishi, T., and Tamaru, K., *Trans. Faraday Soc.* **67,** 3585 (1971).
19. Bowker, M., Houghton, H., and Waugh, K. C., *J. Chem. Soc. Faraday Trans. 1* **77,** 3023 (1981).
20. Noto, Y., Kenzo, F., Takaharu, O., and Tamaru, K., "Advances in Catalysis," Vol. 14, p. 35. Academic Press, New York, 1963.
21. Demuth, J. E., and Ibach, H., *Chem. Phys. Lett.* **60,** 395 (1979).
22. Baudais, F. L., Borschke, A. J., Fedyk, J. T., and Dignam, M. J., *Surf. Sci.* **100,** 210 (1980).
23. Christmann, K., and Demuth, J. E., *J. Chem. Phys.* **76,** 6318 (1982).
24. Sexton, B. A., *Surf. Sci.* **102,** 271 (1981).
25. Foyt, D. C., and White, J. M., *J. Catal.* **47,** 260 (1977).
26. Matsushima, T., and White, J. M., *J. Catal.* **44,** 183 (1976).
27. Stuve, E. M., Madix, R. J., and Sexton, B. A., *Surf. Sci.* **119,** 279 (1982).
28. Bowker, M., and Madix, R. J., *Surf. Sci.* **102,** 542 (1981).
29. Mokwa, W., Kohl, D., and Heiland, G., *Surf. Sci.* **117,** 659 (1982).
30. Golden, D. M., and Benson, S. W., *Chem. Rev.* **69,** 125 (1969).
31. "Atlas of Mass Spectral Data" (Stenhagen, E., Abrahamsson, S., and McLafferty, F. W., Eds.). Interscience, New York, 1969.
32. American Petroleum Institute Research Project 44, Vol. 1. April 30, 1972.